Characterization of Spectral Variations of Irradiated Chicken Breasts with 2D–Correlation Spectroscopy

K. Chao, Y. Liu, Y. R. Chen, D. W. Thayer, W. R. Hruschka

Abstract. *The spectral characteristics of irradiated chicken breasts with dose and storage time were studied by two–dimensional (2D) correlation visible spectroscopy. A Matlab–based 2D–correlation computer program was developed and used to analyze 2D spectra of irradiated chicken meats at various irradiation doses and storage times. The results indicated that the relative amount of oxymyoglobin (560 nm) increases as a result of irradiation. The similarities and differences between the spectral effects at different irradiation doses were also clear, and agreed in general with previously reported spectral changes related to the different forms of myoglobin. The results of the 2D correlation analysis showed that the wavelength region at 560 nm was affected the most during storage. An asymmetric second derivative there showed that highly irradiated meats begin to change approximately 12 days later than raw meats.*

Keywords. *Food safety, Irradiation, Myoglobin, Poultry, Two–dimensional correlation analysis.*

In recent years, U.S. consumers have increased their consumption of poultry products. To ensure a healthy and safe meat supply to the consumers, U.S. legislation requires Food Safety and Inspection Service (FSIS) inspectors inspect each poultry carcass at poultry processing plants. Food safety, in particular the detection and control of food borne pathogens, is an important research area. Treating food with ionizing radiation is broadly effective in controlling food–borne pathogens and reducing the numbers of spoilage organisms (Thayer, 1995 and 1998; Dubey et al., 1998). Research is being conducted to determine the radiation doses that are required to eliminate food–borne pathogens on poultry, red meats, sprouts, and seed without adversely affecting the products.

Irradiation is very effective to eliminate food–borne pathogens to prolong shelf life of various meats and meat products (Grant and Patterson, 1991). Irradiation, however, may alter the color of meats. The radiation effect on color can be influenced by dosage, meat type and packaging methods. In aerobic packages, irradiation decreased the redness of pork and beef, but increased the redness in turkey (Luchsinger et al., 1997; Nanke et al., 1999). In vacuum package, irradiated pork and turkey become redder, but irradiated beef became less red and more yellow (Luchsinger et al., 1996; Nanke et al., 1988). During nonfrozen storage processes, raw meat also undergoes several changes that can affect their quality attributes. These changes are reflected through color, tenderness, and flavor of the meats (Kinsman et al., 1994; Lawrie, 1985). These effects may be due to changes in the composition of the meat tissue caused by the pathogens.

The major pigment composition of meat is in forms of myoglobin. It is primarily responsible for the absorbance in the visible region. Myoglobin can be observed in three different forms on the meat surface. The color of deoxymyoglobin is purplish–red and is a characteristic of recently sliced fresh meat. The color of oxymyoglobin is cherry red and is typical of fresh meat displayed in the supermarket. Metmyoglobin is brownish–red in color and is represented by ferric iron with a water molecular bound at the sixth position. These three forms of myoglobin can inter–convert and may degrade through oxygeneration, oxidation, and reduction reactions when external processes such as storage (Liu et al., 2000) and irradiation are applied.

Visible and near–infrared (Vis/NIR) spectroscopy has been developed for meat identification and to estimate the chemical and physical properties of chicken meat products (Chen et al., 1996; Franke and Solberg, 1971; McElhinney and Downey, 1999). Studies have been successfully conducted on the integrated time–temperature history and physical properties of heat–treated chickens (Chen and Marks, 1998). These studies indicate that Vis/NIR spectroscopy is useful for identification of meats and for quality control of raw and thermally processed poultry products. However, little information on the precise location of the absorbers is available, partly due to the complexity of Vis/NIR spectra.

Two–dimensional (2D) correlation spectroscopy has been adopted as a useful analytical tool in many areas. It can be used to monitor the spectral intensity variation as a function of many variables such as time, temperature, and concentration (Noda, 1993). Recently, the 2D–correlation technique was applied to the study of Vis/NIR spectra of cooked wholesome chicken meats and cold storage (Liu et al., 2000; Liu and Chen, 2000). The results indicated that there are at

Article was submitted for review in August 2001; approved for publication by the Information & Electrical Technologies Division of ASAE in September 2002. Presented at the 2001 ASAE Annual Meeting as Paper No. 013075.

The authors are **Kuanglin Chao**, Research Scientist, **Yongliang Liu,** Visiting Scientist, **Yud–Ren Chen, ASAE Member Engineer,** Research Leader, USDA/ARS/BARC/ISL, Beltsville, Maryland; **Donald W. Thayer,** Research Leader, USDA/ARS/ERRC/Food Safety Unit, Wyndmoor, Pennsylvania; and **William R. Hruschka**, Mathematician, USDA/ARS/BARC/ISL, Beltsville, Maryland. **Corresponding author:** Kuanglin Chao, USDA/ARS/ISL, Building 303, BARC–East, 10300 Baltimore Ave., Beltsville, MD 20705–2350; phone: 301–504–8450; fax: 301–504–9466; e–mail: chaok@ba.ars.usda.gov.

least three dominant visible bands around 445, 485, and 560 nm that are attributable to deoxymyoglobin, metmyoglobin, and oxymyoglobin, respectively.

The USDA/FSIS amended poultry regulations to permit the use of irradiation to treat fresh or frozen uncooked poultry from 1.5 kGy (1 kGy = 1 kiloGray; Gray = 1 joule energy is absorbed per kilogram of matter being irradiated) to 3.0 kGy (USDA, 1992). This article reports the results of applying 2D–correlation spectroscopy to characterize visible spectra of chicken meats irradiated with different dose levels and cold stored for various times. The present 2D–correlation analysis was limited to spectral features of chicken meats in the visible region (400 to 700 nm).

Materials and Methods

Irradiation Processing

De–boned skinless chicken breasts were purchased from a local retailer. The breasts were vacuum–packed with two breasts per air–permeable package (E–300, Cryovac, Deerfield, Ill.). The packages had an approximate oxygen transmission rate of 4000 mL/m^2/24 h at 1 atm at 22.8°C. After packaging, 48 sample packages containing a total of 96 chicken breasts were received frozen and tempered to 0°C for overnight storage before irradiation at 4°C.

Irradiation was conducted at the Food Safety Research Laboratory at USDA/ARS Eastern Regional Research Center (Wyndmoor, Pa.). A Lockheed Georgia Company self–contained ^{137}Cs–gamma irradiation source was used for all exposures. The gamma radiation source consisted of 23 individually sealed source pencils placed in an annular array around a stainless steel cylinder chamber (height × diameter: 63.5 × 22.9 cm). The vacuum–packed chicken breasts were placed within a polypropylene container (4–mm wall) to absorb Compton electrons and used the same sample geometry for irradiation. Samples were placed so that the maximum thickness did not exceed 5.5 cm.

The dose rate provided by the irradiator was 0.10 kGy/min. The temperature was maintained at 4±2°C by a liquid nitrogen gas. Using the constant dose rate, eight target doses (0, 0.2, 0.5, 1.0, 2.0, 3.0, 4.0 and 5.0 kGy) were set for the experiment. Control samples were set for 0 kGy. There were 6 packages (12 samples) of chicken breasts per dose. The actual absorbed doses on chicken breasts were measured by inserting a 5–mm alanine pallet dosimeter into a 104 Electron Paramagnetic Resonance instrument (Bruker Instruments Inc., Billerica, Mass.). Table 1 listed the actual measurement of absorbed doses. In what follows, only the target doses are referred to.

Immediately after irradiation, the chicken breasts were taken out from the radiation chamber. The chicken breast samples were randomly divided into two groups of six samples for each dosage level; one group for Vis/NIR spectral measurement (total of 48 samples) and another (total of 48 samples) for other research.

Table 1. Dose levels and standard deviations for irradiated chicken breasts.

Target Dose (kGy)	Actual Dose (kGy)	Standard Deviation
0.2	0.18	0.01
0.5	0.46	0.02
1.0	0.88	0.04
2.0	1.77	0.07
3.0	2.69	0.19
4.0	3.53	0.23
5.0	4.57	0.26

Vis/NIR Measurement

A spectrophotometer (model 6500, NIRSystems, Silver Spring, Md.) equipped with a rotating cup attachment collected and stored the spectral readings. For each sample, visible to near–infrared spectra (400 to 2498 nm) were collected at 2–nm intervals. Diffuse reflectance readings were calibrated using reflectance measurements from a cermic reference disk. Each spectrum was measured by an average of 32 scans and recorded as 1 log(1/Reflectance) spectrum per sample. The spectra of a total of 48 chicken breasts (six for each dose level) were measured immediately after the irradiation, one spectrum for each chicken breast.

After the initial Vis/NIR measurements, samples were marked according to dose level and sealed in polyethylene bags. Samples were placed in a cooler, filled with ice, and transported to the Instrumentation and Sensing Laboratory (ISL) (within 3 h) for the cold storage experiment. Upon reaching the laboratory, samples were then stored in a cold room at 0°C under constant relative humidity. Approximately every other day up until day 27, samples were taken from the cold room to measure their Vis/NIR spectra.

At the end of the experiment, each set of six spectra for a particular time and dose was averaged. Table 2 lists the average and standard deviation of the spectral absorbance of the six samples at 560 nm, for each dose on measurement day 1. The 104 averaged spectra, corresponding to eight dose levels and 13 measurement times for each dose, were used as raw data.

Data Analysis

2D–Correlation Method

A generalized formalism for the 2D–correlation of data has been developed by Noda (1993). In this treatment, the original data is recast into two orthogonal representations, the synchronous and asynchronous correlation. The synchronous correlation is defined in terms of a discrete summation (Noda, 2000) as:

$$\Phi(\upsilon_1,\upsilon_2)=\frac{1}{m-1}\sum_{j=1}^{m}\tilde{y}_j(\upsilon_1)\,\tilde{y}_j(\upsilon_2) \qquad (1)$$

while the asynchronous correlation is defined as

Table 2. Average and standard deviation of the spectral absorbance of the six samples at 560 nm, for each dose on measurement day 1.

	Mean Absorbance, log (1/R)	Standard Deviation
0.2	0.5312	0.0261
0.5	0.5456	0.0499
1.0	0.5760	0.0605
2.0	0.5809	0.0538
3.0	0.6305	0.0513
4.0	0.5738	0.0675
5.0	0.6187	0.0608

$$\Psi(\upsilon_1,\upsilon_2)=\frac{1}{m-1}\sum_{j=1}^{m}\tilde{y}_j(\upsilon_1)\tilde{z}_j(\upsilon_2) \quad (2)$$

Here, υ_1 and υ_2 are two wavelengths, Φ is the synchronous 2D–correlation value at that pair of wavelengths, m is the number of samples, and $\tilde{y}$ is the dynamic spectrum. Given a set of spectra corresponding to a changing phenomenon, a series of dynamic spectra is calculated by subtracting the average spectrum of the set from each spectrum in the set. In equation 2, Ψ is the asynchronous 2D–correlation value, and the discrete orthogonal spectra $\tilde{z}_j(\upsilon_2)$ can be calculated as:

$$\tilde{z}_j(\upsilon_2)=\sum_{k=1}^{m}N_{jk}\tilde{y}_k(\upsilon_2) \quad (3)$$

where

$$N_{jk}=\begin{cases}0 & if\ j=k\\ 1/[(k-j)\pi] & \text{otherwise}\end{cases} \quad (4)$$

According to the generalized mathematical formalism of Noda, the experimental approach used in 2D–correlation spectroscopy is based on the detection of dynamic spectral variations induced by an external perturbation. In this study, two forms of perturbations are investigated. The first kind of perturbation is the immediate effect of irradiation dose level on fresh meats. The second kind of perturbation is the effect of storage time for each level of irradiated meat. A general form for the spectra can be expressed as a function of wavelength and running index in dose level or storage time.

Based on equations 1 and 2, a 2D–correlation spectral program (twoDcal.m) was implemented using the Matlab software (MathWorks, Natick, Mass.). In computing the synchronous and asynchronous correlation intensities, a 2D matrix of correlation intensities for each pair of wavelengths is developed. These values are then plotted to give a synchronous and an asynchronous correlation maps. Spectral data in ASCII form is input into the program, which then automatically produces the synchronous and asynchronous plots. Interactive input controls the degree of detail in the contour plots and the associated colors.

The axes of the two plots are the wavelength of the first spectral range on the x–axis and the wavelength of the second spectral range on the y–axis. Positive values in the synchronous correlation map are due to spectral bands that are changing in intensity in the same direction, i.e., both increasing. Negative values in the synchronous correlation map are due to spectral bands that are changing in intensity in opposite directions. When the two spectral ranges are the same, a symmetry axis exists along wavelength1 = wavelength2. In the synchronous correlation map, autocorrelation peaks (autopeaks) can be found along this axis while crosspeaks are found in symmetric locations on either side of the symmetry axis. The asynchronous correlation map has no features along the symmetry axis but has oppositely signed crosspeaks in symmetric locations on opposite sides of the axis.

Second Derivative Method

Spectra in the range 400 to 2498 nm were separated into visible (400 to 700 nm) and near–infrared (700 to 1850 nm) region. Spectra in the visible region were used for the study. Each spectrum in the visible region had 151 data points spaced 2 nm apart. Each spectrum was fitted at each point with a Savitzky–Golay (Hruschka, 1987) quadratic polynomial fitting 25 points (12 points on either side). The second derivative of each polynomial at each point was calculated and used as raw data for time dependent analyses. The process resulted in a loss of 12 points on the short wavelength end, reducing the spectrum to 139 points (424 to 700 nm at 2–nm intervals). The Savitzky–Golay algorithm combines a 25–point quadratic smooth with a second derivative, which reduces shifting baseline effects and isolates overlapping peaks.

Results and Discussion

2D–Correlation Analysis

Figure 1 shows the synchronous and asynchronous maps for the 2D calculations of chicken breasts at eight irradiation dose levels. The spectra used to generate the maps are those taken immediately after irradiation. The synchronous map (fig. 1a) is characterized by autopeaks at the diagonal position, observed around 440, 480, and 560 nm. The appearances of the autopeaks indicate that the intensities of these bands change significantly with irradiation dose levels. The sign of the cross peaks (440 vs. 560) or (560 vs. 440 nm) is positive, indicating that the spectral intensity change at the 440–nm band was similar to that at 560 nm. Absorption peaks at these wavelengths are indicative of deoxymyoglobin and oxymyoglobin (Liu and Chen, 2000). The increase of intensities at 460 and 560 nm indicate an accumulation of both deoxymyoglobin and oxymyoglobin species. This finding suggests that irradiation promoted the formation of oxymyoglobin–like pigment and it could be associated with redness in irradiated meats (Bandman, 1987; Clarke and Richards, 1971).

The corresponding asynchronous 2D spectrum shown in figure 1b reveals that the development of the 480–nm absorption is different from those at 440– and 560–nm bands. The negative contour maps suggest that the intensity variation of the 480–nm band occurs at higher dose levels than those of the decrease of the 440– and 560–nm bands. In a study of cooked chicken meats (Liu et al., 2000), it was observed that the intensities at the 440– and 560–nm bands decrease with increasing temperature due to cooking, and that their intensities reduction occurs before the intensity change at 480–nm band. The results strongly suggested that the 440– and 560–nm bands are related to deoxymyoglobin and oxymyoglobin that are easily oxidized and degraded into metmyoglobin (around 480 nm) and other small molecules.

Figure 2 shows synchronous and asynchronous 2D–correlation spectra of non–irradiated chicken meats in cold storage. The 12 spectra used to generate the maps are those with zero dose, excluding the spectra taken immediately after irradiation. In figure 2a, dominant autopeaks at the diagonal position are observed around 440 and 560 nm. The appearances of the autopeaks indicate that the intensities at 440– and 560–nm band change significantly with the storage. A weak autopeak is observed around 510 nm.

The positive cross peaks are found between the 440 nm and the 560 nm, indicating that the spectral intensities at 440 and 560 nm are positively correlated. This suggests a relation between the production or degradation of both

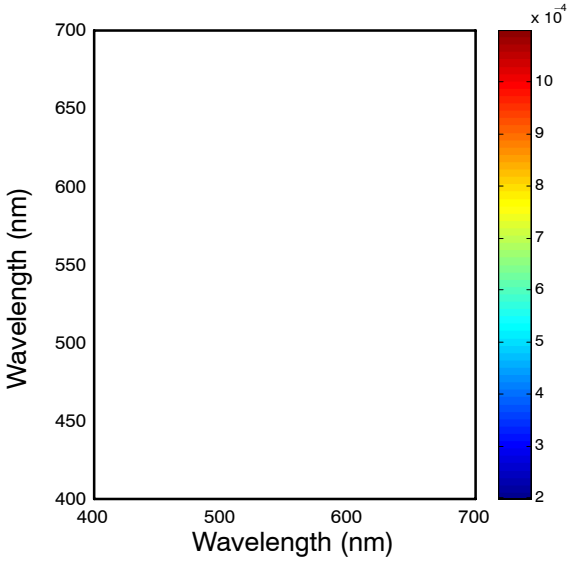

(a)

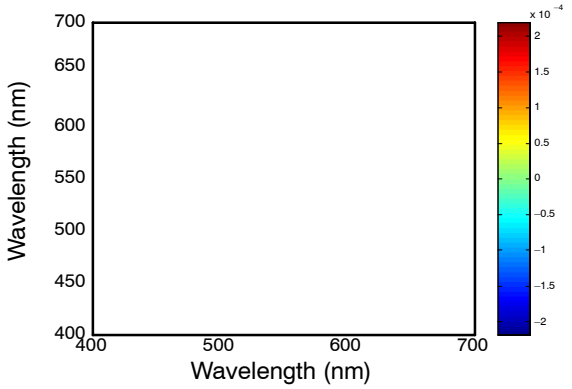

(b)

Figure 1. Synchronous (a) and asynchronous (b) 2D visible correlation spectra of chicken breasts at eight–irradiation dose levels.

deoxymyoglobin and oxymyoglobin species, and it could be linked to discoloration of meat during storage.

The corresponding asynchronous 2D spectrum is shown in figure 2b. Absorption peaks at the 510 and 560 nm are accompanied by several asynchronous cross peaks. The appearance of these cross peaks suggests that the bands at 510 and 560 nm have at least two close but separate bands: 480 and 500 nm for the band at 510 nm, and 570 and 580 nm for the band at the 560 nm. This may be caused by the changes in the secondary structure of myoglobin proteins such as from α–helix to β–sheet (Nabet and Pezolet, 1997) and interactions between proteins and other components such as water and lipids contribute to the variations in the molecular environment of the heme group vibrations.

The development of asynchronous cross peaks (fig. 2b) at 635 nm indicates that the species represented by the 635–nm absorption is different from those species at the 440–, 480–, and 560–nm bands. Liu and Chen (2000) confirmed that the existence of 635–nm band is related to sulfmyoglobin. It is known that one factor leading to meat discoloration during storage is the reaction between H_2S produced by bacterial growth and myoglobin in meat to form sulfmyoglobin (Kinsman et al., 1994; Fennema, 1996).

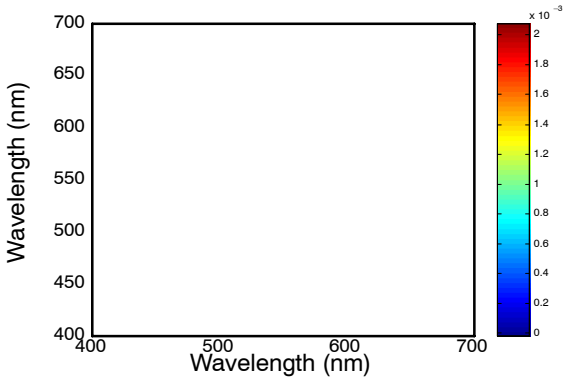

(a)

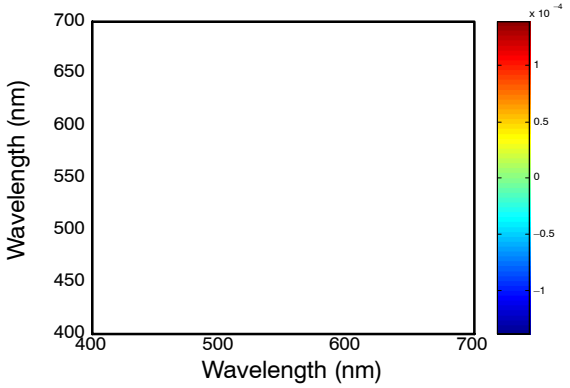

(b)

Figure 2. Synchronous (a) and asynchronous (b) 2D visible correlation spectra of chicken breasts at zero dose during cold storage.

Figure 3 shows synchronous and asynchronous 2D–correlation spectra of irradiated chicken breasts at low dose (1 kGy) level in cold storage. Autopeaks (fig. 3a) are observed at 440, 560, and 605 nm, and cross peaks associated with the autopeaks are also observed at the off–diagonal position. Positive cross peaks (440 vs. 560 nm) and (440 vs. 600 nm) indicate that the spectral intensity change at the 440–nm band was similar to that of the 560 and 605 nm. The appearance of the autopeaks suggests that the intensities of 440, 560, and 605 nm bands vary greatly within low dose irradiated chicken meats. The asynchronous spectrum in figure 3b reveals that the band intensity change around 560 nm occurs differently from the intensity variations in bands around 540 and 575 nm. The spectral intensity changes of the 440–, 540–, 560–, 575–, and 605–nm bands suggest the complexity of degradation/oxidation process of myoglobin species.

Figure 4 shows synchronous 2D–correlation spectra of irradiated chicken meats at high dose (5 kGy) level in cold storage. The most noticeable difference between irradiated and non–irradiated 2D–correlation spectra is the disappearance of the autopeak at 510 nm. It had already begun to disappear in the 1–kGy contour plot, and is now absent entirely. Liu and Chen (2000) mentioned a metmyoglobin band near 500 nm. It is possible that our plot demonstrates a lack of change in the metmyoglobin concentration. The asynchronous plot was similar to the 1 kGy and is not shown.

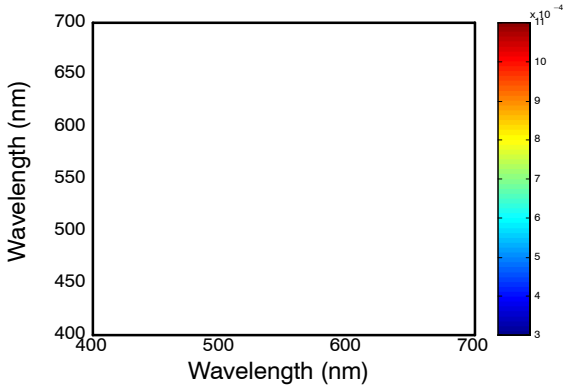

(a)

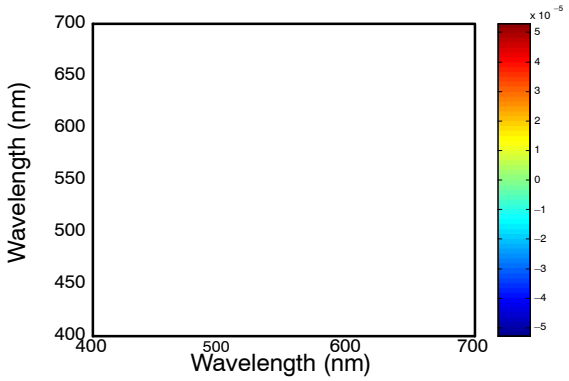

(b)

Figure 3. Synchronous (a) and asynchronous (b) 2D visible correlation spectra of chicken breasts at 1 kGy dose during cold storage.

Derivative Analysis

Figure 5 shows the 12 averaged second derivative control spectra (dose 0) taken after the samples were brought to ISL. Three wavelengths are marked in the 560–nm region, where spectral changes are particularly strong. Two peaks at 548 and 578 nm, which are clearly separated in the early spectra, become one peak at 560 nm as the storage progresses. Tocapture this change quantitatively, an asymmetric second difference was formed from the three wavelengths according to the equation:

$$S''_{560} = S_{560} - 0.4 \times (S_{548} + S_{578}) \quad (5)$$

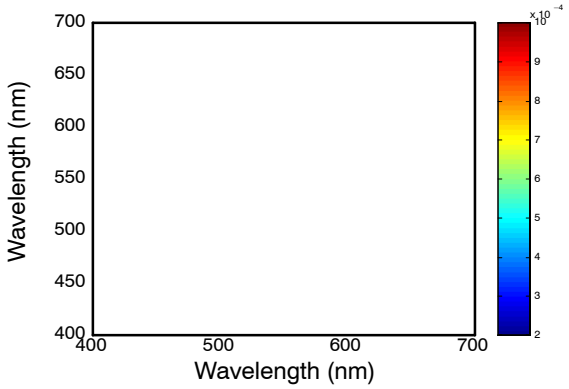

Figure 4. Synchronous 2D visible correlation spectra of chicken breasts at 5 kGy dose during cold storage.

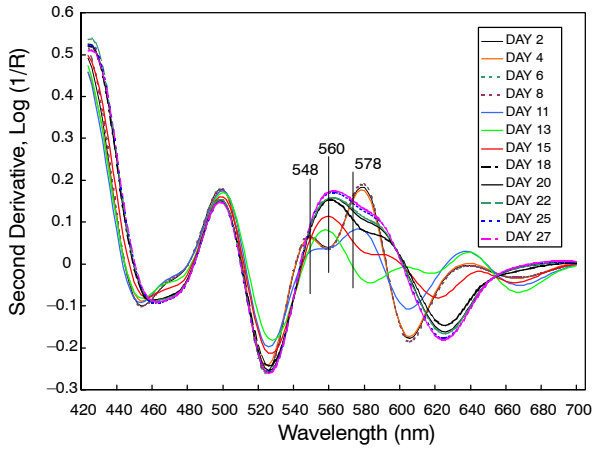

Figure 5. The second derivative visible spectra of non–irradiated chicken breasts during cold storage.

where S_{560} = spectral value at wavelength 560 nm, S" = asymmetric second difference value at wavelength 560 nm.

We noticed the active region around 560 nm by tracing the behavior of the unaveraged derivative spectra of a single sample over time. A particular sample seemed to be in one state in the early days, and then rapidly transformed into another state over a period of about 5 to 8 days. The number of points in the Savitzky–Golay calculation were then adjusted so that the effect seen at 560 nm was a change in the relative intensities of the neighboring peaks, minimizing changes in the wavelengths of peak maxima. This adjustment resulted in the 25–point quadratic fit.

Figure 6 demonstrates the storage effect. The plots are of S''_{560} for different doses over time. The decay effect is a change from one state to another. The position of the change comes later with increased dose level. In more detail, the control samples begin to change at day 8, the 1–kGy samples begin to change at day 16, and the high dose samples begin to change somewhere between 17 and 20 days.

This discovery of equation 5 was guided not only by *de novo* examination of the individual derivative curves. The qualitative information in the 2D plots also suggested the 560–nm region. Activity in this area also agreed with previously reported results (Liu and Chen, 2001) using different preprocessing parameters. A different choice of the number of points in the Savitzky–Golay calculation would result in slightly different wavelengths.

Conclusions

The 2D–correlation analyses are a valuable tool for qualitative analysis of spectral changes over time and other parameters. The 2D–correlation analyses of non–irradiated poultry during cold storage showed interactions between different forms of myoglobin. The intensities of both 440–nm (deoxymyoglobin) and 560–nm (oxymyoglobin) band exhibited significant changes during the cold storage process. The asynchronous 2D visible spectra also illustrated the formulation of sulfmyoglobin (635 nm). These results indicate that

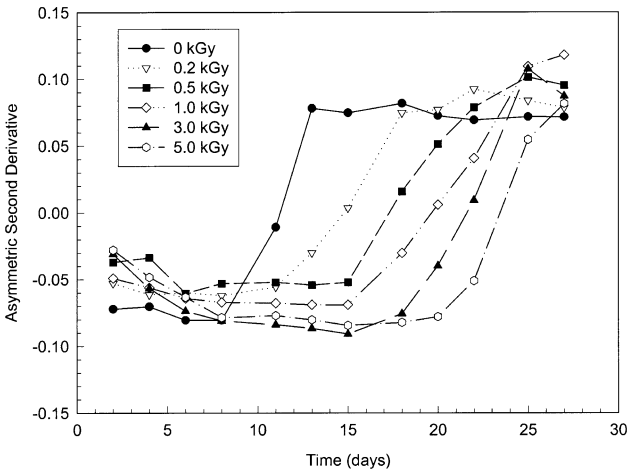

Figure 6. Asymmetric second derivative spectra: five dose levels vs. storage time.

the long–term discoloration of poultry meat is a manifestation of the interaction between different forms of myoglobin.

The similarities and differences between the spectral effects at different irradiation doses were also clear. The known immediate color effects of irradiation (oxymyoglobin at around 560 nm) were easily seen in the 2D plots. Over the long term, the 2D plots showed characteristics similar to those of the non–irradiated breasts. One difference was the disappearance of the band at 510 nm. This effect is usually associated with changes in the secondary structure of myoglobin proteins.

Guided by the 2D–correlation analysis, a wavelength region (560 nm) was found where the storage effect was most evident. This determination involved some experimenting with the parameters involved in derivative calculation. The final result showed clear quantitative differences between the spectral behavior over time (approximately a 12–day delay for high dose) of chicken breasts irradiated at different doses.

Acknowledgements

The authors wish to express their sincere thanks to Dr. Xuetong Fan for his valuable input and technical assistance in making this work possible. We also thank Mr. Robert Schumann of Foss–NIRSystems (Silver Spring, Md.) for the loan of the NIRSystems 6500 spectrophotometer.

References

Bandman, E. 1987. Chemistry of animal tissues: Part I–Proteins. Ch. 3. In *The Science of Meat And Meat Products*, eds. J. F. Price and B. S. Schweigert, 61–101. Westport, Conn.: Food & Nutrition Press, Inc.

Chen, H., and B. P. Marks. 1998. Visible/near–infrared spectroscopy for physical characteristics of cooked chicken patties. *J. of Food Science* 63(2): 279–282.

Chen, Y. R., R. W. Huffman, and B. Park. 1996. Changes in the visible/near–infrared spectra of chicken carcasses in storage. *J. of Process Engineering* 19(2): 121–134.

Clarke, R., and J. F. Richards. 1971. Effects of γ–irradiation on beef myoglobin. *J. of Agric. and Food Chem.* 19(1): 170–174.

Dubey, J. P., D. W. Thayer, C. A. Speer, and S. K. Shen. 1998. Effect of gamma irradiation on unsporulated Toxoplasma gondii oocysts. *International J. of Parasitolology* 28(3): 369–375.

Fennema, O. R. 1996. *Food Chemistry*, 3rd Ed. New York: Marcel Dekker, Inc.

Franke, W. C., and M. Solberg. 1971. Quantitative determination of metmyoglobin and total pigment in an intact meat sample using reflectance spectrophotometry. *J. of Food Science* 36(4): 515–519.

Grant, I. R., and M. F. Patterson. 1991. Effect of irradiation and modified atmosphere packing on the microbiological and sensory quality of pork stored at refrigeration temperature. *International J. of Food Science and Technology* 26(6): 507–519.

Hruschka, W. R. 1987. Data analysis: Wavelength selection methods. In *Near–Infrared Technology in Agricultural and Food Industries*, eds. P. Williams and K. Norris. St. Paul, Minn.: American Association of Cereal Chemists.

Kinsman, D. M., A. W. Kotula, and B. C. Brcidenstein. 1994. *Muscle Foods*, 406–429. New York: Chapman and Hall.

Lawrie, R. A. 1985. *Meat Science*, 4th Ed. Oxford: Pergamon Press.

Liu, Y., and Y. R. Chen. 2000. Two–dimensional correlation spectroscopy study of visible and near–infrared spectral variations of chicken meats in cold storage. *Applied Spectroscopy* 54(10): 1458–1470.

_____. 2001. Analysis of visible reflectance spectra of stored, cooked and diseased chicken meats. *Meat Science* 58(4): 395–401.

Liu, Y., Y. R. Chen, and Y. Ozaki. 2000. Characterization of visible spectral intensity variations of wholesome and unwholesome chicken meats with two–dimensional correlation spectroscopy. *Applied Spectroscopy* 54(4): 587–594.

Luchsinger, S. E., D. H. Kropf, C. M. Garcia Zepeda, M. C. Hunt, J. L. Marsden, E. J. Rubio Canas, C. L. Kastner, W. G. Kuecker, and T. Mata. 1996. Color and oxidative rancidity of gamma and electron beam irradiated boneless pork chops. *J. of Food Science* 61(5): 1000–1005, 1093.

Luchsinger, S. E., D. H. Kropf, C. M. Garcia Zepeda, M. C. Hunt, S. L. Stroda, J. L. Marsden, and C. L. Kastner. 1997. Color and oxidative properties of irradiated ground beef patties. *J. of Muscle Foods* 8(5): 445–464.

Thayer, D. W. 1995. Use of irradiation to kill enteric pathogens on meat and poultry. *J. of Food Safety* 15(3): 181–192. Notes: ERRC No 6200.

Thayer, D. W. 1998. Scientific basis of the Isomedix petition to the FDA to approve the irradiation of meat from domesticated mammalian species. *Proceedings 1997 Meat Industry Research Conference*, 54–56. Chicago, Illinois: AMSA.

USDA, FSIS. 1992. Irradiation of poultry products: Final rule. Federal Register 57: 43588–43600.

McElhinney, J., and G. Downey. 1999. Chemometric processing of visible and near infrared reflectance spectra for species identification in selected raw homogenised meats. *J. of Near Infrared Spectroscopy* 7(3): 145–154.

Nabet, A., and M. Pezolet. 1997. Two–dimensional FT–IR spectroscopy: A powerful method to study the secondary structure of proteins using H–D exchange. *Applied Spectroscopy* 51(4): 466–469.

Nanke, K. E., J. G. Sebranek, and D. G. Olson. 1988. Color characteristics of irradiated vacuum–packed pork, beef, and turkey. *J. of Food Science* 63(6): 1001–1006.

_____. 1999. Color characteristics of irradiated aerobically packaged pork, beef, and turkey. *J. of Food Sci.* 64(2): 272–278.

Noda, I. 1993. Generalized two–dimensional correlation method applicable to infrared, raman, and other types of spectroscopy. *Applied Spectroscopy* 47(9): 1329–1336.

_____. 2000. Determination of two–dimensional correlation spectra using the Hilbert transform. *Applied Spectroscopy* 54(7): 994–999.